Journal of Materials Chemistry B

Accepted Manuscript

ROYAL SOCIETY OF CHEMISTRY

www.rsc.org/materialsB

Cite this: DOI: 10.1039/c0xx00000x

www.rsc.org/xxxxxx

ARTICLE TYPE

Chemiluminescence excited photoelectrochemistry aptamer-device equipped with tin dioxide quantum dots/reduced graphene oxide nanocomposie modified porous Au-paper electrode

Yanhu Wang,[a] Jinmeng Xu,[a] Chao Ma,[a] Shuai Li,[a] Jinghua Yu, [a] Shenguang Ge[b] and Mei Yan, *[a]

Received (in XXX, XXX) Xth XXXXXXXXX 20XX, Accepted Xth XXXXXXXXX 20XX
DOI: 10.1039/b000000x

In this work, a paper-based chemiluminescent excited photoelectrochemical aptamer device was developed for adenosine triphosphate (ATP) measurement based on porous Au-paper electrode modified with tin dioxide quantum dots/reduced graphene oxide nanocomposie (SnO_2 QDs/RGO) integrated with an all-solid-state paper supercapacitor (PSC) amplifier and a digital multi-meter (DMM). Au-paper electrode was constructed through the growth of an gold nanoparticles (AuNPs) layer on the back of paper working electrode to improve the electron conduction. Fe_3O_4@AuNPs nanocomposite were used as labels of luminol, glucose oxidase (GOx) and signal aptamer which greatly enhanced the chemiluminescence emission and provided a simple magnetic separation approach to attain interference-free measurement for real detection. GOx was used for the oxidation of glucose to produce H_2O_2 which not only used as the co-reactant in the CL system, but also as the electron donors to suppress the corrosion of SnO_2 QDs under illumination as well as to facilitate the generation of stable photocurrent. A PSC was constructed and integrated into the PPECD as an effective electrical energy storage unit to collect and store the photocurrents. And the stored electrical energy could be released instantaneously through a low cost, portable, and simple DMM to obtain an amplified current for the quantification of ATP.

Introduction

Microfluidic paper-based analytical devices (μ-PADs) have attracted more and more attention in the past years due to their advantages such as low cost, easy operation, disposability, and potential to be made in mass production.[1, 2] To date, scientific and technical thrust about analytical methods on μ-PADs has been directed toward the construction of electrochemical and luminescent methods.[3-5]

Adenosine triphosphate (ATP) is the major energy source within the cell to drive a number of biological processes as well as a marker for cell viability because it is present in all metabolically active cells and its concentration declines very rapidly when the cells undergo necrosis or apoptosis.[6] And great efforts have been devoted to ATP detection based on aptasensors,[7, 8] such as fluorescent,[9] electrochemical,[10] colorimetric,[11] chemiluminescent (CL)[12] and electrochemiluminescent (ECL)[13] methods. While each strategy has distinct advantages, each also presents its own unique set of limitations, such as poor sensitivity and high equipment cost.

Photoelectrochemical (PEC) measurement as a newly developed technique for the detection of biomolecules, has attracted substantial research scrutiny for its desirable sensitivity and hence better analytical performances.[14-16] Different from ECL[17, 18] and CL[19] analysis, which detect the optical signal produced from analyte-intervenient electrochemical and chemical reactions, respectively, the PEC analysis uses a beam of excitation light to induce the detectable photoelectron transfer between photoelectrochemical-active species and electrode. [20] This newly emerged technique has promising analytical potential for a low-cost, simple, portable, rapid, and high-through put assay on μ-PADs for point-of care diagnosis.

Recently, some metal oxide semiconductor nanoparticles such as ZnO, TiO_2, and quantum dots (QDs) have been used as significant photoelectrochemical cells. Among various semiconductor nanomaterials, tin dioxide quantum dots (SnO_2 QDs) as an ideal material which are important owing to their potential applications based on gas sensing,[21] field emission,[22] electrochemical,[23] photocatalytic,[24] and photovoltaic properties,[25, 26] has been extensively used as optical labels or electrochemical tracers for following biorecognition events and biocatalytic transformations because of their desirable features such as broad excitation and symmetric tunable emission spectra, photochemical stability and binding compatibility with biomolecules.[27] Meanwhile, for photovoltaic devices, the incorporation of reduced graphene oxide (RGO) as an advanced nanoelectrocatalyst for constructing electrochemical sensors owing to its extraordinary electronic transport properties, large surface area, and high electrocatalytic activities can enhance the charge-separation and facilitate charge-transport, and thus improve the photovoltaic performance.[28, 29] Herein, in this work a nanocomposite of SnO_2 QDs and RGO was prepared by one-pot reaction as the photoelectrochemical probe (SnO_2 QDs/RGO) for the measurement of photocurrent.

However, in all the conventional PEC methods, to measure the weak photocurrents sensitively, an electrochemical workstation is

needed which limited its wide spread, made the instrument complicated and also departed from the portable and low-cost trend for μ-PADs. Hence, a strategy for substitution of the electrochemical workstation is highly deserved. The paper electronics,[30-33] as one of the most ancient technologies of humankind and display a modern appearance, have been demonstrated. The paper supercapacitor [34] a state-of-the-art circuit component that can temporarily store a large amount of electrical energy and release it when needed, has attracted much attention due to its high electrical energy storage, long life cycle, and fast charging-discharging rate. Herein, in this work, an all-solid-state paper supercapacitor (PSC) was constructed and integrated into the PEC device as an effective electrical energy storage unit to collect and store the photocurrents. The stored electrical energy could be released instantaneously through a low-cost, portable, and simple digital multimeter (DMM) to obtain an amplified current.[35] Thus, in this work, a paper-based PEC device (PPECD) intergrated with a PSC was designed and fabricated. To further enhance the sensitivity of PEC assay, gold nanoparticles (Au NPs) modified paper electrode (Au-PWE) with high conductivity and surface area with high conductivity and surface area was employed as the working electrode to obtain a high photocurrent through the further acceleration of electron transfer in the paper sample zone.[36]

To further develop a simple, low-cost, and portable PEC assay on μ-PAD, a chemiluminescent (CL) excited PEC analytical protocol was designed by luminol-H_2O_2-*p*-iodophenol (PIP) CL system as the luminescence donor. Here PIP was a CL intensifier. H_2O_2 produced by the oxidation of glucose in the presence of glucose oxidase (GOx) was not only used as the co-reactant in the CL system, but also as the electron donors to suppress the corrosion (lattice dissolution) of SnO_2 QDs under illumination as well as to facilitate the generation of stable photocurrent. Fe_3O_4@AuNPs was used as a carrier of luminol, GOx and signal aptamer (ssDNA2) which greatly enhanced the CL emission and provided a simple magnetic separation approach to attain interference-free measurement for real detection. This design greatly simplified the analytical apparatus and realized physical light source-free photoelectrochemical detection.[20]

In this work, we have successfully developed a methodology for low-cost, simple, rapid, portable, disposable, and sensitive ATP which was employed as a proof-of-concept analyte because the sandwich ATP-binding aptamers were readily available for it detection on μ-PADs using SnO_2 QDs/RGO modified Au-PWE as the working electrode, a PSC as the current-amplifier, and a DMM as the terminal current detector. Using luminol, GOx and ssDNA2 functionalized Fe_3O_4@AuNPs as signal probe and capture aptamer (ssDNA1) bound SnO_2/RGO modified Au-PWE as the aptasensor, the proposed method showed excellent performance, acceptable sensitivity, low detection limit, wide linear concentration range, good stability and reproducibility. The presence of RGO and the Au-PWE greatly improved the photocurrent transfer efficiency. This PPECD will be very useful when the level of an analyte in real complex biological sample for simple, rapid, low-cost point-of-care testing in remote regions, developing or developed countries.

Experimental section

Materials

The aptamer, split into two oligonucleotides, was purchased from Sangon Biotech Co., Ltd. (Shanghai, China), and the sequences of the two oligonucleotides were as follows:

(1) ssDNA1: 5′-NH2–TTTTTTTTTTACCTGGGGGAGTAT-3′;

(2) ssDNA2: 5′-TGCGGAGGAAGGTTTTTT–SH-3′.

Adenosine triphosphate (ATP), cytidine triphosphate (CTP), guanosine triphosphate (GTP), and uridine triphosphate (UTP) were purchased from Aladdin Chemistry Co. Ltd. Whatman chromatography paper #1 (200.0 mm×200.0 mm) (pure cellulose paper) was obtained from GE Healthcare Worldwide (Pudong Shanghai, China) and used with further adjustment of size. Ultrapure water obtained from a Millipore water purification system (≥18 MΩ, Milli-Q, Millipore) was used in all assays and solutions. Poly(dimethyldiallylammonium chloride) (PDDA) (20%, w/w in water, molecular weight = 200000-350000), Poly(vinyl alcohol) (PVA), sodium dodecyl sulfate (SDS), *p*-iodophenol (PIP), and glucose oxidase (GOx) were purchased from Alfa Aesar. Tetrachloroauric acid ($HAuCl_4$) as the precursor for the formation of AuNPs was purchased from Shanghai Sangon Biological Engineering Technology & Services Co. Potassium ferricyanide, graphite powders, hydroxylamine hydrochloride and sodium citrate were products from Shanghai Chemical Reagent Co. All other reagents were of analytical grade and used as received.

Preparation of SnO_2 QDs/RGO Nanocomposie, Au NPs, Fe_3O_4, and Fe_3O_4@Au NPs

Graphene oxide was first prepared by a modified Hummers' method.[37] Then the SnO_2 QDs/RGO nanocomposite was synthesized using the following one-step wet chemical method according to previous work.[38] Namely, 0.1 g of the dried graphene oxide was added into 500 mL of ultrapure water. The obtained mixture was sonicated for 90 min. At the same time, 2.4 g of $SnCl_4{\cdot}5H_2O$ was dissolved into 20 mL of ultrapure water and then 8 mL of the graphene oxide solution was added in which the concentration of $SnCl_4$ is about 0.24 M. The above mixture was stirred for 5 h and then centrifuged for 5 min at 8000 $r{\cdot}min^{-1}$. In order to improve the crystallinity of the SnO_2 QDs and remove the residual water molecules and functional groups from the graphene oxide, the product was heated at 500 ℃ for 2 h under an argon atmosphere. For comparison, the single SnO_2 QDs and reduced graphene oxide (RGO) were synthesized using the same process except the addition of the aqueous dispersion graphene oxide and $SnCl_4{\cdot}5H_2O$.

Au NPs were synthetized by sodium citrate reductionof $HAuCl_4$ in water.[39] Briefly, 2.5 mL of 1% sodium citrate was rapidly added to 100 mL of boiling 0.01% $HAuCl_4$ solution under vigorous stirring, and then the solution changed colour from pale-yellow to wine-red. Boiling continued for 10-15 min, and then the heating source was removed. The colloids were stirred for another 15 min and cooled to room temperature. After cooling, the synthesized Au NPs was centrifuged at 12000 rpm for 20 min and then re-dissolved in 10 mL 1mM SDS. After that the

concentrated Au NPs were stored at 4 ℃ for further use. Fe_3O_4@AuNPs nanoparticles were prepared by a two-step method according to the procedures.[40] First, the synthesis of Fe_3O_4 seeds was prepared by the chemical co-precipitation of Fe^{2+} and Fe^{3+} ions (2:1 molar ratio) in alkaline medium. NaOH solution (2 mol/L) was added to $FeCl_3$ and $FeCl_2$ under vigorous agitation at 50 ℃. During the reaction process, the pH value was maintained at about 10. The solution was then heated at 80 ℃ for 1 h under a N_2 atmosphere. Finally, the resulting precipitate was separated by magnetic decantation and washed with ultrapure water. Second step involved the synthesis of Fe_3O_4@AuNPs nanoparticles prepared by the reduction of Au^{3+} using Fe_3O_4 particles as seeds. Under constant stirring, 100 mL of sodium citrate (2.29 g/mL) was prepared and heated at 90 ℃. Then, 40 mg of Fe_3O_4 was immediately added to the solution. About 5 mL of $HAuCl_4$ solution (0.01mol/L) was added and heated for 15 min before cooling to room temperature with vigorous stirring for 15–20 min. The obtained core–shell Fe_3O_4@AuNPs were separated from free gold nanoparticles by an external magnet and redispersed in ultrapure water, then stored in a refrigerator at 4 ℃ prior to use.

Preparation of ssDNA2/luminol/Fe_3O_4@AuNPs/GOx labels

The bioconjugates were freshly prepared by addition of luminol (30 mmol/L, 500 μL), ssDNA2 (50 μM, 50 μL) and GOx (10 $\mu g \cdot mL^{-1}$, 100 μL) into Fe_3O_4@AuNPs nanoparticles (2 mL) by sonication for 2 h. After magnetic separation, the prepared ssDNA2/luminol/Fe_3O_4@Au NPs/GOx labels were resuspended in PBS (pH=7.4) and stored at 4℃ before use.

Construction of the paper working electrode

The preparation of paper working electrode is illustrated in Scheme S2. The porous Au-PWE was fabricated through growth of an Au NPs layer on the back of cellulose fibers in the paper sample zone of PEC tab to enhance the conductivity and enlarge the effective surface area of bare PWE according to the method described in our previous works.[36, 41] The as-prepared Au-PWE on the PEC tab was then modified through the addition of SnO_2/RGO nanocomposite onto the surfaces of the Au-coated cellulose fibers in the paper sample zone. Briefly, an aliquot of 10 μL of the mixture was cast onto the surface of the porous Au-PWE by layer-by-layer with PDDA as the first layer. The SnO_2 QDs/RGO nanocomposite modified porous Au-PWE was thoroughly rinsed with ultrapure water, and then the solvent was evaporated at room temperature to obtain the SnO_2 QDs/RGO nanocomposite film modified electrode.

Measurement procedure of this PPECD

As shown in Scheme S2, the PPECD was constructed by immobilizing the corresponding ssDNA1 (10 μL, 1 μM) on the SnO_2 QDs/RGO/Au-PWE through the addition of PDDA and kept it for 1 h. Then they were rinsed with PBS (pH=7.4, 0.01 M) carefully to remove the excess ssDNA1. Then, the ssDNA1/SnO_2 QDs/RGO/Au-PWE was blocked by the BSA solution for 0.5 h to cover the possible remaining active sites. After rinsed with PBS, the resulting PPECD was stored at 4 ℃ before use. To carry out the CL excited PEC measurement, the aptasensor was first incubated with sample solutions (10 μL) containing different concentration of ATP which subsequently incubated with ssDNA2/luminol/Fe_3O_4@AuNPs/GOx solution, then washing thoroughly with PBS for preventing the nonspecific binding and achieving the best possible signal-to-background ratio. Prior to PEC detection, the PEC tab was folded and stacked above the supercapacitor tab as indicated in Scheme 1B. The folded PPECD was then clamped (Scheme 1C) between the two compatibly designed circuit boards (Scheme 1C (a) and (b)) and put into a model cassette (Scheme 1D). Thereafter, the clamped PPECD was connected to the DMM through the conductive connector on the circuit boards (Scheme 1D).

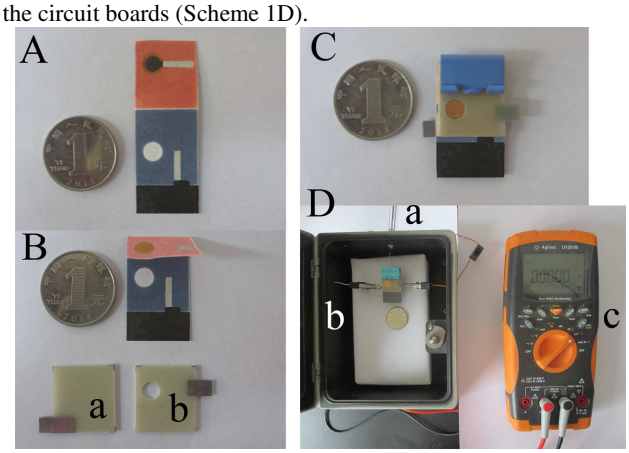

Scheme 1 Assay procedures of this PPECD. (A) Picture of the prepared PPECD; (B) the PEC tab was folded above the supercapacitor tab; (B) the timer tab was folded above the PEC tab, (a) (b) picture of the circuit boards used in this work; (C) the folded PPECD was clamped by the circuit boards. (D) The clamped PPECD was put into the cassette and connected with the DMM: (a) micro-syringe, (b) cassette, (c) DMM.

The CL reaction was triggered after the solution of glucose and PIP dropped into the modified Au-PWE by a pipette, in the presence of GOx, the glucose could be oxidized to generate H_2O_2, and the luminol reacted with the H_2O_2 and PIP in solution to yield a CL emission to excite SnO_2 QDs to generate photocurrent for the determination of ATP (shown in Scheme 2). The generated photocurrent was collected between the modified Au-PWE on PEC tab and the carbon counter electrode on supercapacitor tab to charge the PSC. A high instantaneous current through the DMM was obtained once the switch was closed. And the concentration of ATP was quantified by the intensity of current response.

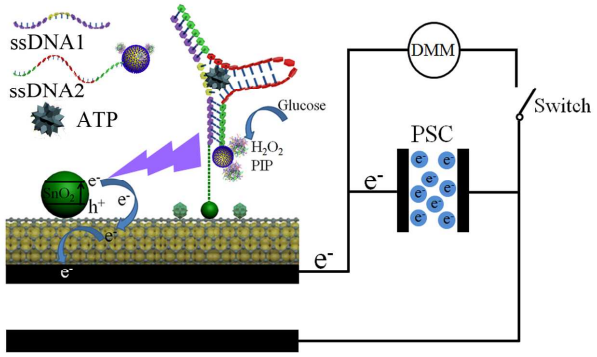

Scheme 2 Schematic illustration of the photocurrent generation mechanism in the modified paper sample zone of the Au-PWE under the CL light source.

Results and discussion

Characterization of this PPECD

This PPECD was fabricated on pure cellulose paper. The porous structures and microfibers of the pure cellulose paper are shown in Fig. 1A. Meanwhile, SEM was used to determinate the morphology of the cellulose fibers after the growth of the Au NPs layer on the surface of cellulose fibers (Fig. 1B). After the growth of Au NPs, the Au NPs seeds were rapidly enlarged by incubating in the growth solution under the self-catalytic reduction mechanism of Au NPs growth. Finally, a continuous and dense conducting AuNPs layer with interconnected Au NPs was obtained completely on the cellulose fiber surfaces growth.

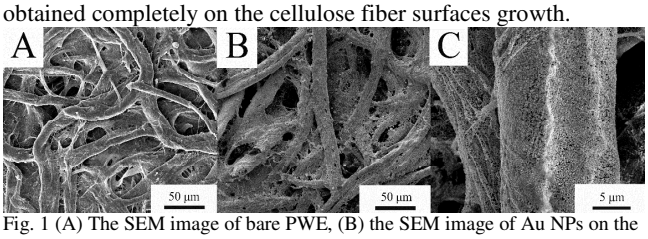

Fig. 1 (A) The SEM image of bare PWE, (B) the SEM image of Au NPs on the surfaces of the cellulose fibers in PWE, (C) SEM image of the enlarged Au-PWE.

Characterization of SnO_2 QDs, RGO and SnO_2/RGO nanocomposite

The morphology of SnO_2 QDs, RGO and their nanocomposites was observed on the Transmission Electron Microscopy (TEM) (shown in Fig. 2). In Fig. 2A, it is apparent that the SnO_2 QDs are ultra-fine and the particle size of these nanoparticles is about 3 nm. Fig. 2B showed that the graphene was single layer structure with smooth surface, no defect or hole could be observed on the basal plane. The well conjugated structure could benefit the electronic conductance, and was desirable to construct an electrochemical biosensing platform. TEM was used to further characterize the appearance of SnO_2 QDs/RGO nanocomposite, as shown in Fig. 2C, a graphene sheet was coated with lots of homogeneous and dense SnO_2 QDs having highly uniform size. Meanwhile, the XRD and UV-VIS (Fig. 3) have also been used to confirm the successful preparation of SnO_2 QDs, RGO and their nanocomposites.

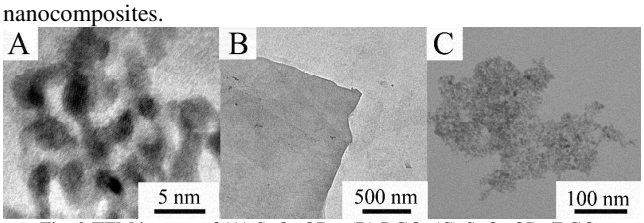

Fig. 2 TEM images of (A) SnO_2 QDs, (B) RGO, (C) SnO_2 QDs/RGO.

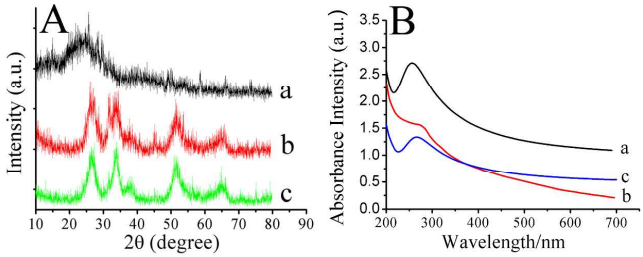

Fig. 3 (A) XRD and (B) UV-VIS of RGO (a), SnO_2 QDs (b), and SnO_2 QDs/RGO.

EIS characterization of the modified PPECD

Electrochemical impedance spectroscopy (EIS) is an effective method to monitor the changes of interfacial properties, allowing the understanding of chemical transformation and processes associated with the conductive electrode surface.[42] To further confirm the successful construction of the PPECD, the EIS of the resulting paper working zones is shown in Fig. 4. Electrochemical impedances of the PEC sensor were performed with addition of a background solution of 5.0 mM $Fe(CN)_6^{4+/3+}$ containing 0.1 mM KCl, and the frequency range is at 100 mHz to 10 kHz at 220 mV.

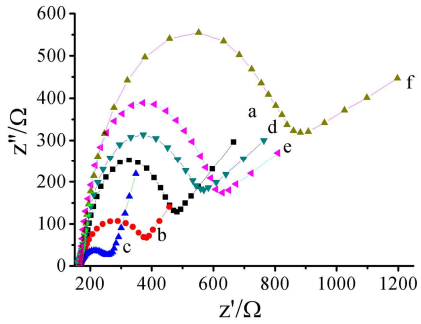

Fig. 4 EIS of the PWE under different condition in 10.0 mM $[Fe(CN)_6]^{3+/4+}$solution containing 0.5 M KCl: (a) bare PWE, (b) Au-PWE, (c) ssDNA1 modified Au-PWE, (d) ssDNA1 modified Au-PWE after the addition of ssDNA2 in absence of ATP, (f) ssDNA1 modified Au-PWE after the addition of ssDNA2 in presence of ATP.

Fig. 4 shows the Nyquist plot of impedance for the stepwise modification process on the Au-PWE. The EIS of bare PWE showed a relatively small Ret value (curve a). After the growth of an Au NPs layer on the back of the PWE, a much lower resistance was obtained (curve b), implying that the Au NPs is an excellent electric conducting material and accelerated the electron transfer. After modification with SnO_2 QDs/RGO nanocomposite (curve c), the semicircle domain with Ret value further decreased, suggesting the promotion of electron transfer process at the modified electrode surface. Remarkable increase in the R_{et} value was observed after the immobilization of the immobilization of ssDNA1 (curve d), indicating that the negatively charged biomolecule increased the electron-transfer distance. After being incubated with the solution of ssDNA2 in the absence of ATP, only little amount of ssDNA2 were captured in the PWE through physical adsorption with ssDNA1, thus the electron-transfer kinetics of the redox probe was slow down slightly (curve e). The obvious increase of R_{et} from curve e to curve f could be attributed to the formation of stable and nearly insulating sandwich composites layer through the ssDNA2/luminol/Fe_3O_4@AuNPs/GOx labels combination on the surfaces of Au-coated cellulose fibers.

Photocurrent generated mechanism of the PPECD

The photocurrent generation mechanism of the proposed PPECD is shown in Scheme 2, and could be described as follow. The glucose could be reacted with O_2 in the presence of GOx to produce gluconicacid and H_2O_2. While the generated H_2O_2 could immediately react with luminol and PIP, then yield a CL emission. Under the illumination of the CL emission, SnO_2 QDs were photo-excited to produce an electron (e^-)–hole (h^+) pair. The injection of the conduction-band (CB) electrons into the carbon

working electrode through RGO attached to the AuNP layer yield the photocurrent, whereas the electron donor (H_2O_2) provided the electrons to the valence-band (VB) holes to thus complete the photocurrent generation cycle.

Due to the long durability of the CL emission from luminol-H_2O_2-PIP system, the resulting photocurrents could maintain for 500 s.[12] Therefore, herein the PSC could be charged stably by the photocurrent generated from the PWE for 60 s. Then, the PSC was short connected through a low-cost and hand held DMM with the Max/Min function, which could record and display the maximum value of measurements after pressing the Max/Min button once. Thus, the instantaneous amplified current from the PSC could be obtained.

Photoelectrochemistry performance of the aptasensor

In a further control experiment, to verify the formation of RGO and the growth of Au NPs layer on the back of cellulose fibers could improve photocurrent transfer efficiency and electron transfer between SnO_2 QDs and electrode surface for the measurement of photocurrent, a contrast test under an external light source has been provided in this work, which will be conducive to demonstrate that RGO and the formation of Au NPs layer could improve photocurrent transfer efficiency and electron transfer perfectly. The photocurrent responses of SnO_2/PWE, SnO_2/Au-PWE, and SnO_2/RGO/Au-PWE were recorded in Fig. 5A. The photocurrent of the SnO_2/RGO/Au-PWE (a) increased evidently compared to that of the SnO_2/Au-PWE (b) and SnO_2/PWE (c). This may result from the conjugation effect of RGO, which could improve the electron-transfer and increased the photocurrent. Meanwhile, through the growth of an Au NPs layer on the back of cellulose fibers with higher capability of electron transfer, could effectively shuttle electrons from the base electrode surface to the surface of SnO_2 QDs and made the PEC sensor more stable. Furthermore, the photocurrent response from this PPECD was directly related to the amount of the immobilized ssDNA2/luminol/Fe_3O_4@AuNPs/GOx, which depended on the concentration of ATP. Thus, a greater amount of ATP captured in the Au-PWE can lead to a higher current response (shown in Fig. 5B). To verify the signal amplification of Fe_3O_4@AuNPs, a comparison test was carried out. As shown in Fig. 5B, curve c and d were the photocurrent response generated from ssDNA2/luminol/Fe_3O_4@AuNPs/GOx and ssDNA2/luminol/@AuNPs/GOx respectively. Compared with AuNPs used as signal label, the Fe_3O_4@AuNPs used as the signal amplifier could obtain an enhanced photocurrent response.

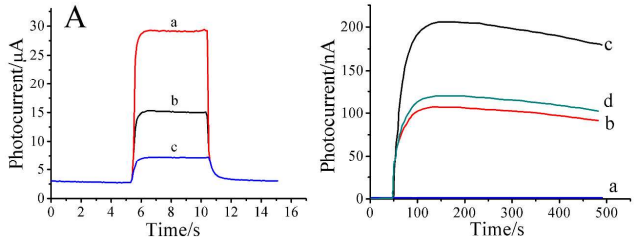

Fig. 5 Photocurrent response of (a) SnO_2/RGO/Au-PWE, (b) SnO_2/Au-PWE, and (c) SnO_2/PWE under an external light source. (C) Photocurrent response of capture aptamer (ssDNA1)/SnO2/RGO/Au-PWE in the presence of 0 (a), 10 pM (b) and 10 nM (c) ATP with an internal CL light source; photocurrent response of the proposed aptasensor using ssDNA2/luminol/Fe_3O_4@AuNPs/GOx (c) and ssDNA2/luminol/@AuNPs/GOx (d) as signal amplifier containing 10 nM ATP, respectively.

Optimization of detection conditions

The hybridization process was performed online at room temperature in the paper sample zone of SnO_2 QDs/RGO/Au-PWE. The photocurrent intensity for 1.0 nM ATP increased quickly with the increase of hybridization time and then levelled off, indicating the maximum formation of the sandwich complexes in SnO_2 QDs/RGO/Au-PWE (Fig. 6A). Hence, considering the optimal analytical performance and development of this method for high sample throughput, the hybridization time of 150 s was selected. Meanwhile, the effect of detection solution pH on the current intensity of the PPECD was displayed in Fig. 6B. In the examined pH range, the maximum current response of this PPECD occurred when pH was 7.4. Taking into account the bioactivity of immune-reagents, a pH 7.4 PBS was selected as the detection solution.

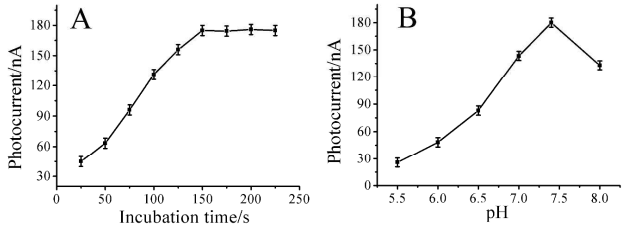

Fig. 6 (A) Effect of incubation time (A) and pH (B) on the photocurrent intensity.

Analytical performance

Under the optimum conditions, the results showed that both the photocurrent generated directly from the prepared PPECD (I_{PWE}) and the amplified current released from the PSC (I_{PSC}) increased linearly with the logarithmic concentration of ATP (0.1pM-100nM, Fig. 7). The linear regression equations were I_{PWE}(nA)=168.98+35.35lgcATP(nM) and I_{PSC}(nA)=2196.81+459.58lgcATP(nM) with a correlation coefficient of 0.9937 and 0.9968 respectively, and the limits of detection at a signal-to noise ratio of 3 was 0.025 pM (defined as S/N=3), which was mainly attributed to the concomitant amplification of the background photocurrent from the modified PWE, indicative of acceptable quantitative behavior.

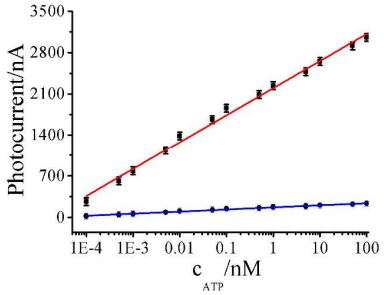

Fig. 7 Relationship between current response and concentration of ATP with (red) and without (blue) the amplification of the paper supercapacitor.

The analytical reliability and application of this PPECD was evaluated by assaying clinical serum samples using the proposed method and showed acceptable reliability and accuracy (Table S1). The results gave the relative standard deviation (RSD) to be less than 4.5%, and the recoveries are between 97.8% and

103.4%, indicating an acceptable veracity of this method. Hence, the developed PPECD provided a possible application for the detection of ATP in clinical diagnostics.

Evaluation of selectivity reproducibility and stability of this PPECD

Selective is a crucial analytical parameter in determining the specificity, and reliability, of a multiplex immunoassay. To assess the specificity of the developed method for the detection of ATP, experiments were performed by using three other ATP analogues in human serum: cytidine triphosphate (CTP), guanosine triphosphate (GTP), and uridine triphosphate (UTP). As shown in Fig. 8, GTP, UTP or CTP did not exhibit major photocurrent signal change as compared to that of ATP. This result agrees with the fact that the aptamer is specific toward ATP, and may become a general method for any aptamer of interest.

The reproducibility of this PPECD for ATP was investigated with inter-assay precision. The RSD for the parallel detections of 0 M, 50 pM, and 1.0 nM ATP with ten prepared PPECD was 3.12%, 2.75%, and 2.91%, respectively. When the prepared PPECD was stored and measured at intervals of 3 days, no obvious change was observed after 5 weeks under ambient conditions. These results indicated that this proposed PPECD had better reproducibility, stability, and precision during manufacture, storage or long-distance transport to remote regions and developing countries compared with previous antibody-based paper immunodevice.[43, 44]

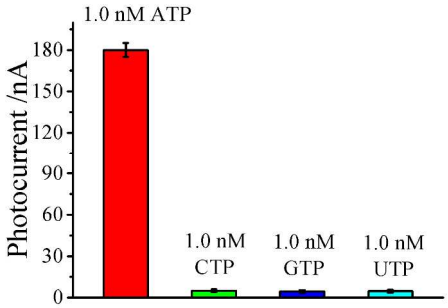

Fig. 8 Selectivity of this proposed PPECD to ATP.

Conclusions

In this work, a truly low-cost, simple, portable, and disposable PPECD based on a CL-excited PEC assay and integrated paper supercapacitor was presented. The paper supercapacitor, as well as the SnO_2 QDs/RGO modified Au-PWE, is very efficient in photocurrent enhancement and amplification to produce the amplified current required for the read-out in DMM. Fe_3O_4@AuNPs was used as the carrier which greatly enhanced the CL emission and provided a simple magnetic separation approach to attain interference-free measurement for real detection. The proposed PPECD providing a low-cost, simple, portable, and disposable approach for detection and diagnosis in developing countries, resource-limited and remote regions and allowing the expensive and sophisticated electrochemical workstation or lock-in amplifier to be abandoned. In conclusion, this low-cost, simple, portable, and highly sensitive current amplification strategy could be used as a powerful and potential tool for current related analysis on μ-PADs, and we believe its applications will continue to expand in the fields of clinical and diagnosis.

Acknowledgements

This work was financially supported by National Natural Science Foundation of China (21277058, 21175058, 51273048); Natural Science Foundation of Shandong Province, China (ZR2012BZ002).

Notes and references

[a]*Key Laboratory of Chemical Sensing & Analysis in Universities of Shandong, University of Jinan, Jinan 250022, China. Fax: 55 +86-531-82765959; Tel: +86-531-82767161; E-mail: ujn.yujh@gmail.com.*
[b]*Shandong Provincial Key Laboratory of Preparation and Measurement of Building Materials, University of Jinan, Jinan 250022, China.*

Electronic Supplementary Information (ESI) available: See DOI: 10.1039/b000000x/

1 A. W. Martinez, S. T. Phillips and G. M. Whitesides, Anal. Chem., 2010, 82, 3-10;.
2 H. Liu and R. M. Crooks, J. Am. Chem. Soc., 2011, 133, 17564-17566.
3 E. Carrilho, S.T. Phillips, S.J. Vella, A.W. Martinezand and G.M. Whitesides, Anal. Chem., 2009, 81, 5990–5998.
4 W. Dungchai, O. Chailapakul and C.S. Henry, Anal. Chem., 2009, 81, 5821–5826.
5 J.L. Delaney, C.F. Hogan, J. Tian and W. Shen, 70 Anal. Chem., 2011, 83, 1300–1306.
6 L. M. Verstraeten, K. D. Coninck, K. Vlassak, W. Verstraete, H. Werf and M. Ilaiwi,Soil Biol. Biochem., 1983, 15, 397–402.
7 D. E. Huizenga and J. W. Szostak,Biochemistry, 1995,34, 656–665.
8 J. Shi, T. G. Cha, J. C. Claussen, A. R. Diggs, J. H. Choi and D. M. Porterfield, Analyst, 2011, 136, 4916–4924.
9 Z. W. Tang, P. Mallikaratchy, R. H. Yang, Y. M. Kim, Z. Zhu, H. Wang and W. H. Tan,J. Am. Chem. Soc., 2008,130, 11268–11269.
10 X. Zuo, Y. Xiao and K. W. Plaxco,J. Am. Chem. Soc., 2009, 131, 6944–6945.
11 J. Wang, L. Wang, X. Liu, Z. Liang, S. Song, W. Li, G. Li and C. Fan,Adv. Mater., 2007, 19, 3943–3946.
12 S. S. Zhang, Y. M. Yan and S. Bi, Anal. Chem., 2009, 81, 8695–8701.
13 W. Yao, L. Wang, H. Y. Wang, X. L. Zhang and L. Li,Biosens. Bioelectron., 2009, 24, 3269–3274.
14 Y. Dilgin, L. Gorton, and G. Nisli, Electroanalysis, 2007, 19, 286-293.
15 H. B. Yildiz, R. Freeman, R. Gill, and I. Willner, Anal. Chem., 2008, 80, 2811-2816.
16 E. Golub, G. Pelossof, R. Freeman, H. Zhang, and I. Willner, Anal.Chem., 2009, 81, 9291-9298.
17 L. L. Li, K. P. Liu, G. H. Yang, C. M. Wang, J. R. Zhang and J. J. Zhu, Adv. Funct. Mater., 2011, 21, 869-878.
18 L. Ge, J. X. Yan, X. R. Song, M. Yan, S. G. Ge and J. H. Yu, Biomaterials, 2012, 33, 1024-1031.
19 R. Freeman, X. Q. Liu and I. Willner, J. Am. Chem. Soc. , 2011,133 ,11597-11604.
20 W. W. Tu, W. J. Wang, J. P. Lei, S. Y. Deng and H. X. Ju, Chem. Commun., 2012, 48, 6535–6537.
21 L. Xiao, H. Shen, R. Von Hagen, J. Pan, L. Belkoura and S. Mathur, Chem. Commun., 2010, 46, 6509-6511.
22 T. T. Baby and S. Ramaprabhu, J. Appl. Phys., 2012, 111, 34311-34315.
23 H. Ahn, H. Choi, K. Park, S. Kim and Y. Sung, J. Phys. Chem. B, 2004, 108, 9815-9820.
24 T. Jia, W. Wang, F. Long, Z. Fu, H. Wang and Q. Zhang, J. Phys. Chem. C, 2009, 113, 9071–9077.
25 S. Gubbala, V. Chakrapani, V. Kumar and M. K. Sunkara, Adv. Funct. Mater., 2008, 18, 2411–2418.

26 N. Kudo, Y. Shimazaki, H. Ohkita, M. Ohoka and S. Ito, Sol. Energy Mater. & Sol. Cells, 2007, 1243–1247.
27 C. H. Jiang, E. Hosono and H. S. Zhou, Nanotoday, 2006, 1, 28-33.
28 X. M. Zhao, S. W. Zhou, L. P. Jiang, W. H. Hou, Q. M. Shen and J. J. Zhu, Chem. Eur. J., 2012, 18, 4974–4981.
29 J. Shi, H. Y. Zhang, A. Snyder, M. X. Wang, J. Xie, D. M. Porterfield and L. A. Stanciu, Biosens Bioelectron, 2012, 38, 314–320.
30 L. B. Hu, J. W. Choi, Y. Yang, S. Jeong, F. La Mantia, L. F. Cui and Y. Cui, Proc. Natl. Acad. Sci. U. S. A., 2009, 106, 21490-21494.
31 V. L. Pushpar aj, M. M. Shaijumon,A. Kumar, S. Mu rugesan, L. Ci, R. Vajtai, R. J. Lin hardt, O. Nalamasu and P. M. Ajayan, Proc. Natl. Acad. Sci. U. S. A., 2007, 104, 13574-13577.
32 A. D. Mazzeo, W. B. Kalb, L. Chan, M. G.Killian, J. F. Bloch, B. A. Mazzeo and G. M. Whitesides, Adv. Mater., 2012, 24, 2850-2856.
33 F. Eder, H. Klauk, M. Halik, U. Zschieschang, G. Schmid and C. Dehm, Appl. Phys. Lett., 2004, 84, 2673-2675.
34 L. Yuan, X. Xiao, T. Ding, J. Zhong, X. Zhang, Y.Shen, B. Hu, Y. Huang, J. Zhou and Z. L. Wang, Angew. Chem., Int. Ed., 2012, 90 51, 4934–4938.
35 L. Ge, P. P. Wang, S. G. Ge, N. Q. Li, J. H. Yu, M. Yan and J. D. Huang, Anal. Chem., 2013, 85, 3961–3970.
36 Y. H. Wang, L. Ge, P. P. Wang, M. Yan, S.G. Ge, N. Q. Li, J. H. Yu and J. H. Huang, Lab Chip, 2013, 13, 3945-3955.
37 W. S. Hummers and R. E. Offeman, J. Am. Chem. Soc.1958, 80, 1339-1339.
38 Y. Wei, C. Gao, F. L. Meng, H. H. Li, L. Wang, J. H. Liu, and X. J. Huang, J. Phys. Chem. C, 2012, 116, 1034–1041.
39 G. Frens, Nature: Physical Science, 1973, 241, 20–22.
40 J. P. Li and H. L. Gao, Electroanalysis, 2008, 20,881−887.
41 J. X. Yan, L. Ge, X. R. Song, M. Yan, S. G. Ge and J. H. Yu, Chem. Eur. J., 2012, 18, 4938-4945.
42 S. M. Park and J. S. Yoo, Anal. Chem., 2003, 75, 455–461.
43 D. J. Zang, L. Ge, M. Yan, X. R. Song and J. H. Yu, Chem. Commun.， 2012, 48, 4683–4685.
44 P. P. Wang, L. Ge, M. Yan, X. R. Song, S. G. Ge, J. H. Yu, Biosens. Bioelectron., 2012, 32, 238–243.

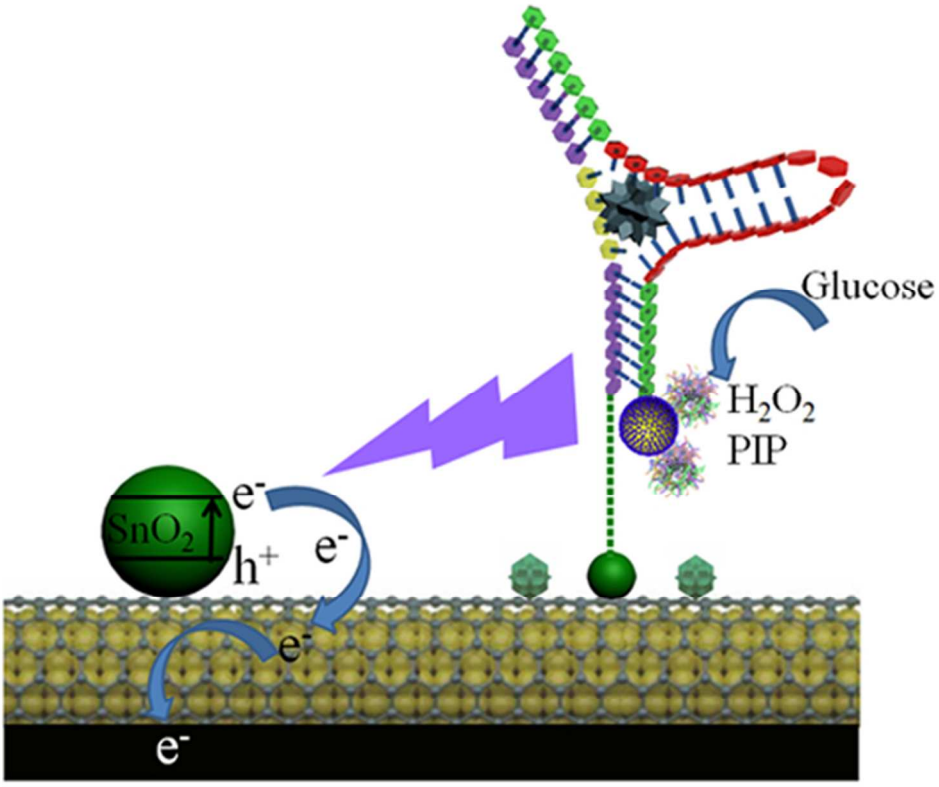

63x51mm (300 x 300 DPI)